Fusion reactions in Lab

In lab-made fusion we use reactions with larger cross-sections:

D + D $\rightarrow$ T (1.01 MeV) + p (3.02 MeV)

$\rightarrow$ ^{3}He (0.82 MeV) + n (2.45 MeV)

D + ^{3}He $\rightarrow$ ^{4}He (3.6 MeV) + p (14.7 MeV)

D + T $\rightarrow$ ^{4}He (3.5 MeV) + n (14.1 MeV)

T + T $\rightarrow$ ^{4}He + 2 n + 11.3 MeV

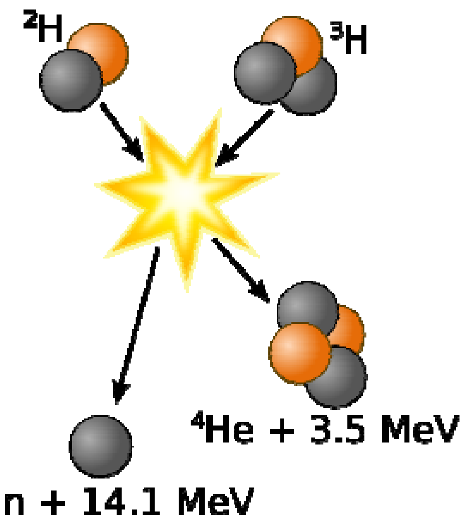

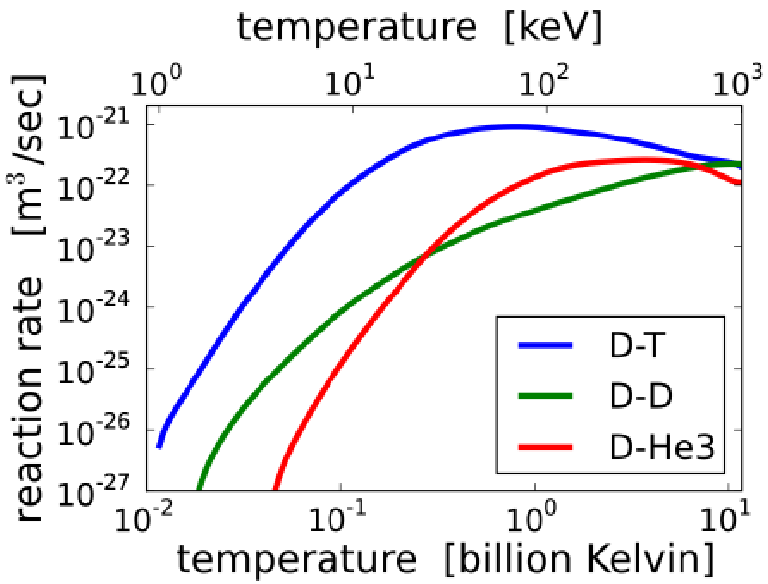

Cross-sections: parameterisation

S-function represents slowly varying nuclear part of the fusion reaction probability

S-function is important for fitting cross-section to experimental data:

$$\sigma = \frac{S(E)}{E \exp(B_G / \sqrt{E})}$$

S-function is calculated with R-matrix cross-section analysis and fitted with a Padé polynomial:

$$S(E) = \frac{A1 + E(A2 + E(A3 + E(A4 + EA5)))}{1 + E(B1 + E(B2 + E(B3 + EB4)))}$$

R-matrix theory is a mathematical description and a parameterisation of nuclear reactions: a many-body nuclear system with a short range strong forces is treated as a system with only 2-body degrees of freedom outside the 'channel radii'.

(Wigner, Eisenbud *Phys.Rev.***72***(1947)29* and Lane, Thomas *Rev.Mod.Phys.***30***(1958)257)*

Cross-sections: parameterisation (2)

List of parameters for fusion cross-sections

Coefficient	$T(d,n)^4He$	$^3He(d,p)^4He$	$D(d,p)T$	$D(d,n)^3He$
B_G ($\sqrt{keV}$)	34.3827	68.7508	31.3970	31.3970
A1	6.927×10^{4}	5.7501×10^{6}	5.5576×10^{4}	5.3701×10^{4}
A2	7.454×10^{8}	2.5226×10^{3}	2.1054×10^{2}	3.3027×10^{2}
A3	2.050×10^{6}	4.5566×10^{1}	-3.2638×10^{-2}	-1.2706×10^{-1}
A4	5.2002×10^{4}	0.0	1.4987×10^{-6}	2.9327×10^{-5}
A5	0.0	0.0	1.8181×10^{-10}	-2.5151×10^{-9}
B1	6.38×10^{1}	-3.1995×10^{-3}	0.0	0.0
B2	-9.95×10^{-1}	-8.5530×10^{-6}	0.0	0.0
B3	6.981×10^{-5}	5.9014×10^{-8}	0.0	0.0
B4	1.728×10^{-4}	0.0	0.0	0.0
Energy range (keV)	0.5–550	0.3–900	0.5–5000	0.5–4900
$(\Delta S)_{max}$ (%)	1.9	2.2	2.0	2.5

E in keV; cross sections in mb ≡ 10^{-27} cm^2

Bosch, Hale *Nuclear Fusion 32(1992)611*

Cross-sections

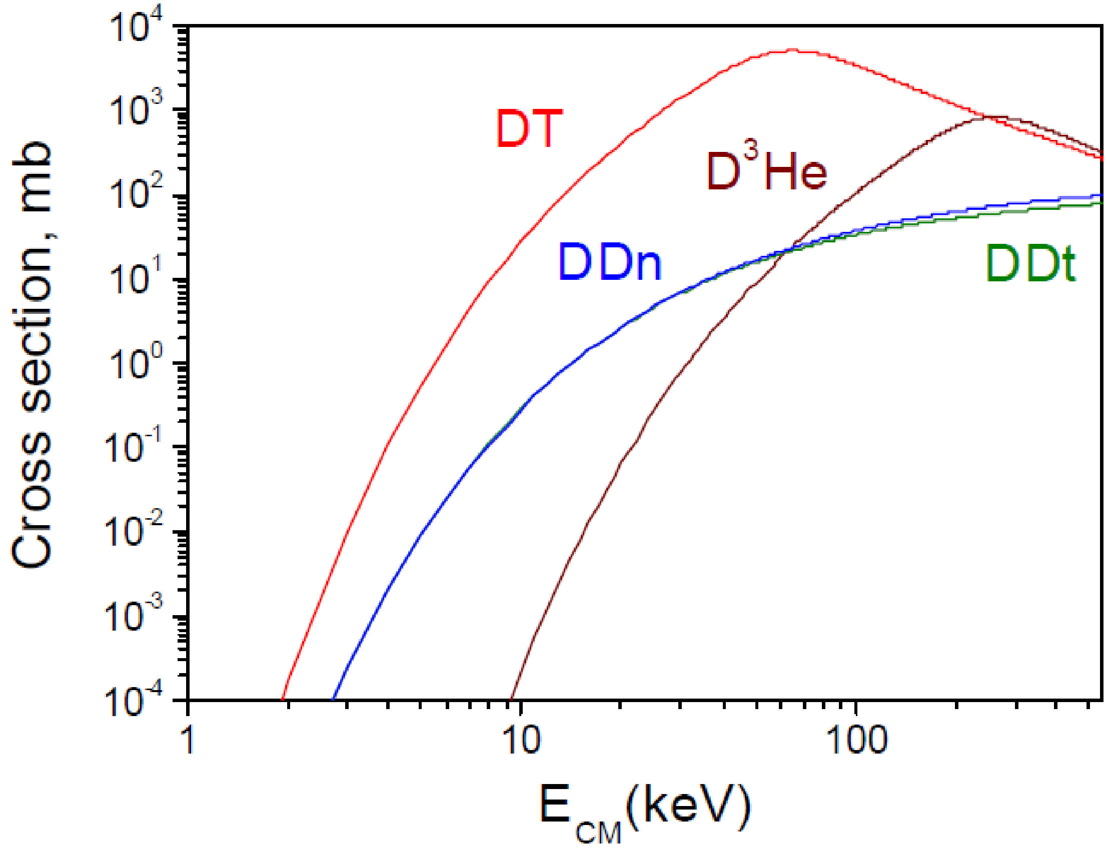

Cross-sections: fusion reactivity parameterisation

In plasma, ions have a velocity distribution, $f(\vec{V})$

and fusion rate is proportional to fusion reactivity : $R = \frac{n_i n_j}{1+\delta_{ij}} \langle \sigma v \rangle$

n_i, n_j – ion densities; fusion reactivity - $\langle \sigma v \rangle = \iint f(\vec{V}_1) f(\vec{V}_2) \sigma(|\vec{V}_1 - \vec{V}_2|) |\vec{V}_1 - \vec{V}_2| d\vec{V}_1 d\vec{V}_2$

Useful parameterisation for the fusion reactivites:

$$\langle \sigma v \rangle = C1\theta \sqrt{\xi / (\mu c^2 T^3)}\, e^{-3\xi}$$

$$\theta = T \Big/ \left[1 - \frac{T(C2 + T(C4 + TC6))}{1 + T(C3 + T(C5 + TC7))} \right]$$

$$\xi = (B_G^2 / (4\theta))^{1/3}$$

Peres *Nucl.Mater.50(1979)5569*

Cross-sections: fusion reactivity parameterisation (2)

List of parameters for fusion reactivities in Maxwellian plasmas

Coefficient	$T(d,n)^4He$	$^3He(d,p)^4He$	$D(d,p)T$	$D(d,n)^3He$
B_G ($\sqrt{keV}$)	34.3827	68.7508	31.3970	31.3970
m_rc^2 (keV)	1 124 656	1 124 572	937 814	937 814
C1	1.17302×10^{-9}	5.51036×10^{-10}	5.65718×10^{-12}	5.43360×10^{-12}
C2	1.51361×10^{-2}	6.41918×10^{-3}	3.41267×10^{-3}	5.85778×10^{-3}
C3	7.51886×10^{-2}	-2.02896×10^{-3}	1.99167×10^{-3}	7.68222×10^{-3}
C4	4.60643×10^{-3}	-1.91080×10^{-5}	0.0	0.0
C5	1.35000×10^{-2}	1.35776×10^{-4}	1.05060×10^{-5}	-2.96400×10^{-6}
C6	-1.06750×10^{-4}	0.0	0.0	0.0
C7	1.36600×10^{-5}	0.0	0.0	0.0
T_i range (keV)	0.2–100	0.5–190	0.2–100	0.2–100
$(\Delta\langle\sigma v\rangle)_{max}$ (%)	0.25	2.5	0.35	0.3

T is in keV; reactivity is in cm^2s^{-1}

Bosch, Hale *Nuclear Fusion 32(1992)611*

Cross-sections: fusion reactivity

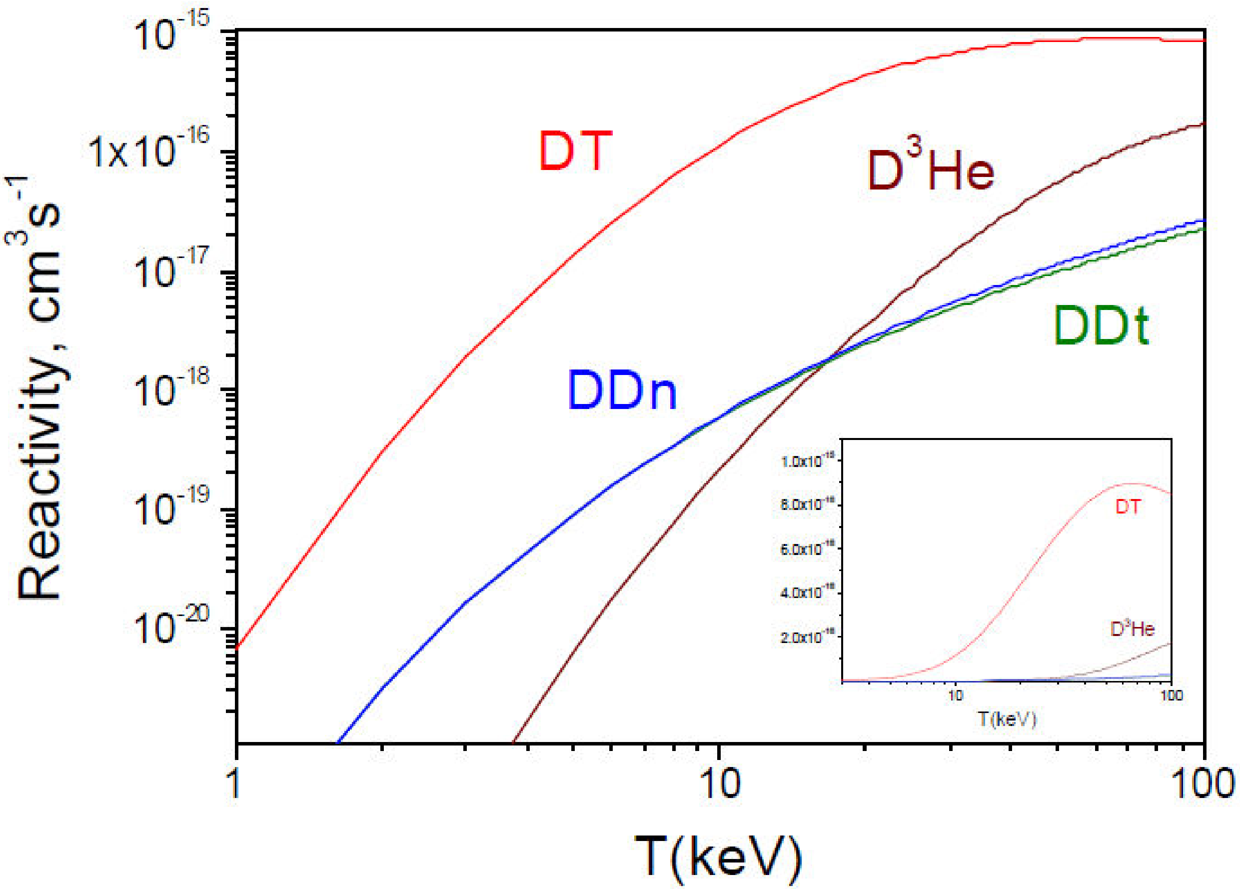

$$@T = 67keV$$

$$\langle \sigma v \rangle_{DT} = \max$$

$$@T = 17keV$$

$$\langle \sigma v \rangle_{D^3He} = \langle \sigma v \rangle_{DDn}$$

$$@T = 90keV$$

$$\frac{\langle \sigma v \rangle_{D^3He}}{\langle \sigma v \rangle_{DDn}} \approx 6.5$$

Fusion γ -ray emission profile

Fusion α-particle source can be measured with radiation capture reaction – branch of the main fusion reactions D+T = α + n and D+^{3}He = α + p :

D + T → ^{5}He + γ (Q=16.63 MeV) and

D + ^{3}He → ^{5}Li + γ (Q=16.38 MeV)

The branching ratio is small: $$\frac{\sigma(\gamma)}{\sigma(\alpha+n)} \approx \frac{\sigma(\gamma)}{\sigma(\alpha+p)} \approx 5\times10^{-5}$$

Nevertheless, the γ-ray profile measurements are feasible for the ITER-like reactors.

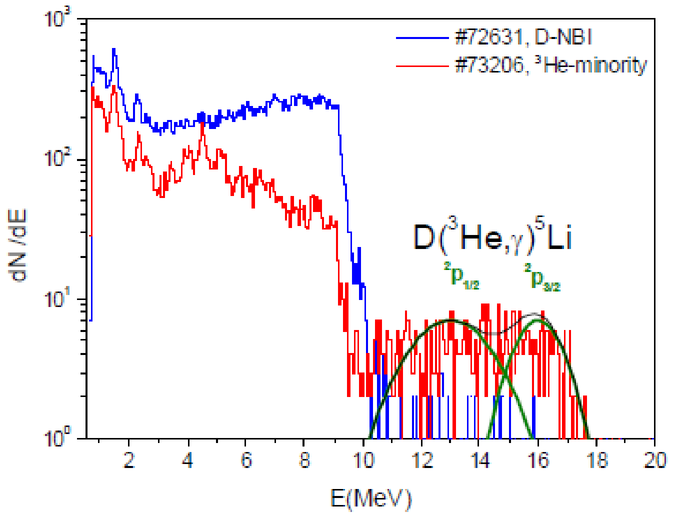

The gamma-ray spectrum recorded in the JET discharge with ^{3}He-minority heating of the D-plasma.

2 broad peaks are related to the different final states in ^{5}Li nucleus.

Gamma-ray diagnostics: γ - spectra

γ-ray spectrum recorded in D(^{3}He)-plasmas

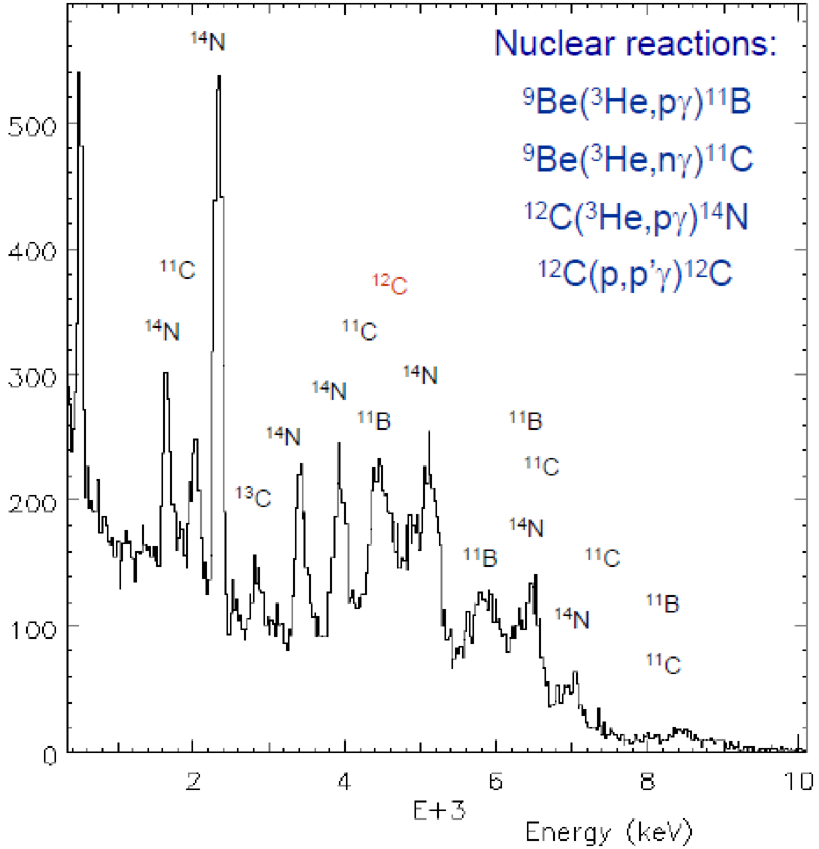

γ-ray spectra recorded in α-particle simulation experiment:

^{4}He- and D-ions accelerated in MeV-energy range with 3rd harmonic ICRF

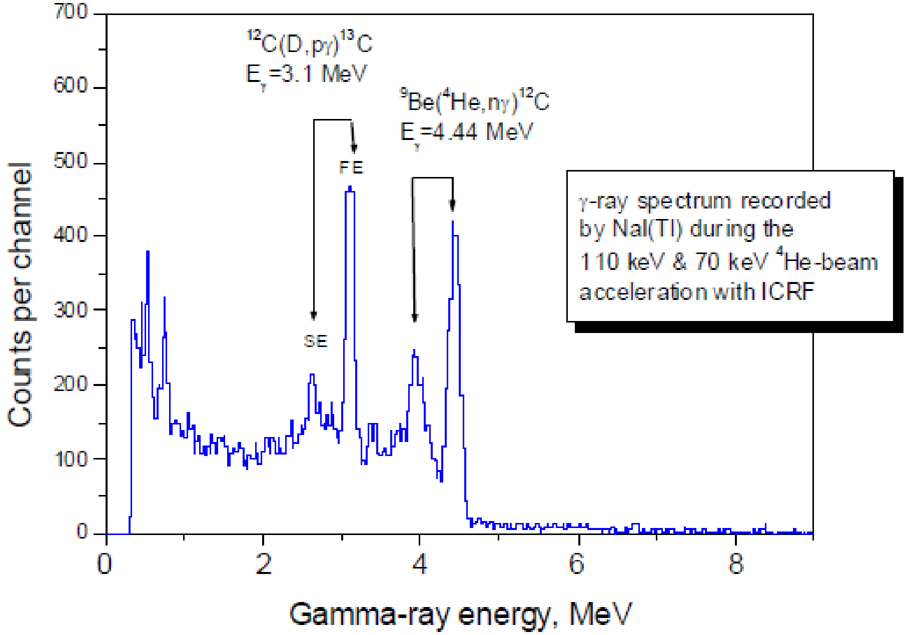

Gamma-ray diagnostics: ^{4}He acceleration experiments

monotonic q-profile

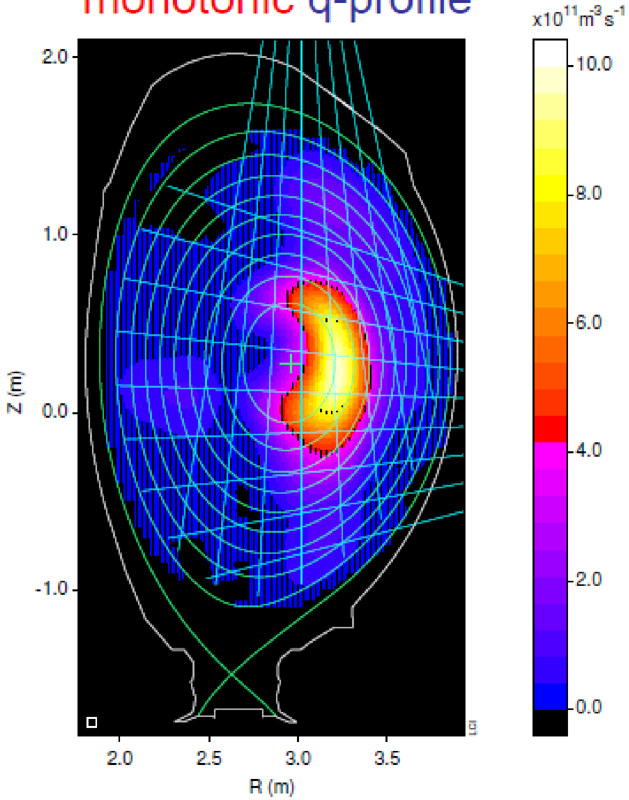

non-monotonic q-profile

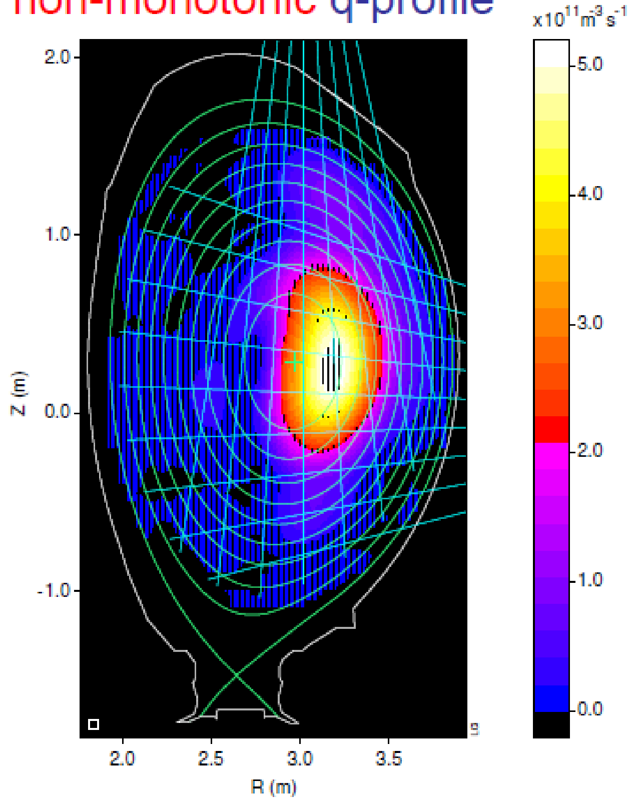

Tomographic reconstructions of profiles measured in different q-profile phases of the optimised shear plasma discharge. The monotonic q-profile was settled down after sawtooth crash.

Diagnostic reactions

The goal is to study

- Fusion reaction products: *n, p, t, ^3He* and α
- ICRF-driven ions: *H, D, T, ^3He* and *^4He* (in JET)

Neutron diagnostics: 2.5-MeV neutrons from DD-reaction and 14-MeV from DT

Gamma diagnostics: fast ions

γ -ray emission is produced due to nuclear reactions with fuel and with the main JET (and ITER) impurities, Be and C

protons	deuterons	tritons	^{3}He
$D(p,\gamma)^3He$	$^9Be(d,p\gamma)^{10}Be$	$T(d,\gamma)^5He$	$D(^3He,\gamma)^5Li$
$T(p,\gamma)^4He$	$^9Be(d,n\gamma)^{10}B$	$^9Be(t,n\gamma)^{11}B$	$^9Be(^3He,p\gamma)^{11}B$
$^9Be(p,\gamma)^{10}B$	$^{12}C(d,p\gamma)^{13}C$	$^{12}C(t,\gamma)^{15}N$	$^9Be(^3He,n\gamma)^{11}C$
$^9Be(p,p'\gamma)^9Be$		$^{12}C(t,n\gamma)^{14}N$	$^9Be(^3He,d\gamma)^{10}B$
$^9Be(p,\alpha\ \gamma)^6Li$		$^{12}C(t,\alpha\gamma)^{11}B$	$^{12}C(^3He,p\gamma)^{14}N$
$^{12}C(p,p'\gamma)^{12}C$			

α-particle diagnosis in JET is based on the $^9Be(\alpha,n\gamma)^{12}C$ reaction

Cross-section measurements are needed

Nuclear reaction	Energy range, MeV	Levels, MeV	Angular distributions	Comments
$^{12}C(^{3}He,p\gamma)^{14}N$	0.7, 1.0, 2.5, 3, 4-6	1, 2, 4, 5, 6, 7, 8	p, γ	Validation of existing data. Optimal number of angles: p - 5 , γ - 4 (e.g. 0^0,55^0,90^0,150^0)
$^{9}Be(^{3}He,p\gamma)^{11}B$	0.5-6	1, 2, 6	p, γ	Optimal number of angles, AD for strong lines
$^{9}Be(^{3}He,n\gamma)^{11}C$	0.5-6	1-9	n, γ	Optimal number of angles, AD for strong lines
$^{9}Be(^{3}He,d\gamma)^{10}B$	0.5-6	1-7	d, γ	Optimal number of angles, AD for strong lines
$^{12}C(d,p\gamma)^{13}C$	0.5-1	1,2,3	p, γ	There is a paper of F.Papillon, P.Walter (NIM/B,132,468,1997). I have not got the paper, check the AD for L1.
$^{9}Be(d,n\gamma)^{10}B$	0.3-3	1-7	n, γ	Optimal number of angles, AD for strong lines, 0.3-1 MeV band is very important, ITER relevant.
$^{9}Be(d,p\gamma)^{10}Be$	0.3-3	1, 2, 4	p, γ	Optimal number of angles, AD for strong lines, 0.3-1 MeV band is very important, ITER relevant.
$^{9}Be(d,\gamma)^{11}B$	0.3-1	-	γ_0	0.3-1 MeV band is very important, ITER relevant.
$^{9}Be(t,n\gamma)^{11}B$	TBD			Validation of existing data. $^{9}Be(t,\gamma)^{12}B$ could be interesting at low energies

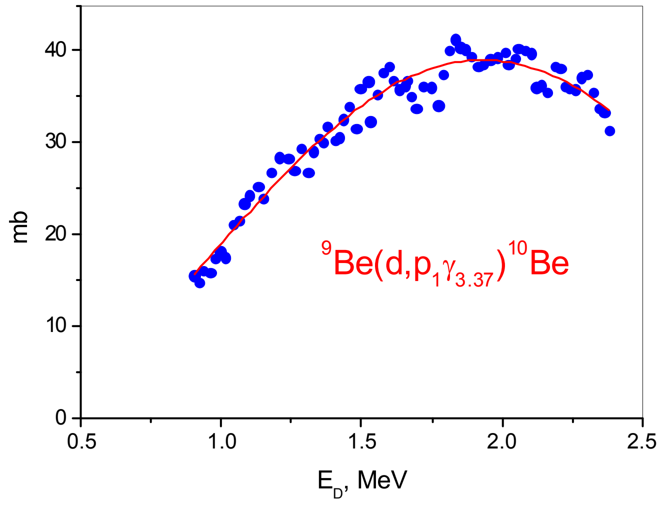

mb
$^{9}Be(d,p_1\gamma_{3.37})^{10}Be$
E_D, MeV

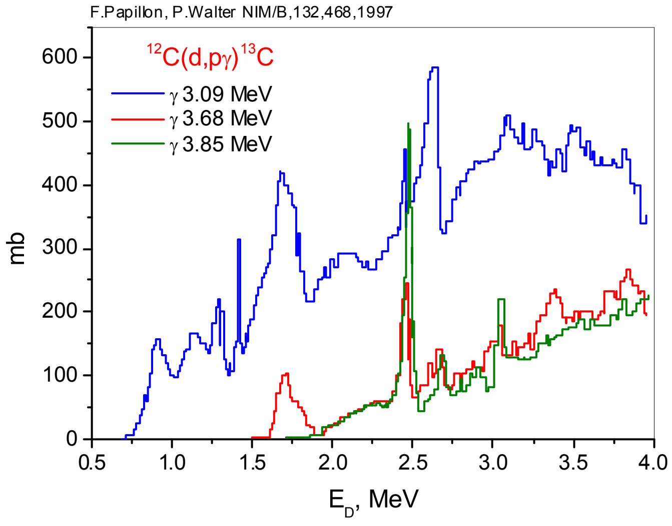

F.Papillon, P.Walter NIM/B,132,468,1997
$^{12}C(d,p\gamma)^{13}C$
γ 3.09 MeV
γ 3.68 MeV
γ 3.85 MeV
mb
E_D, MeV

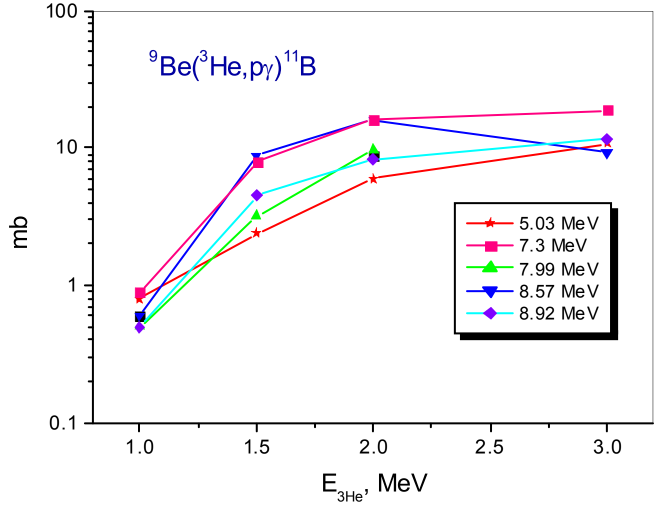

$^{9}Be(^{3}He,p\gamma)^{11}B$
5.03 MeV
7.3 MeV
7.99 MeV
8.57 MeV
8.92 MeV
mb
E_{3He}, MeV

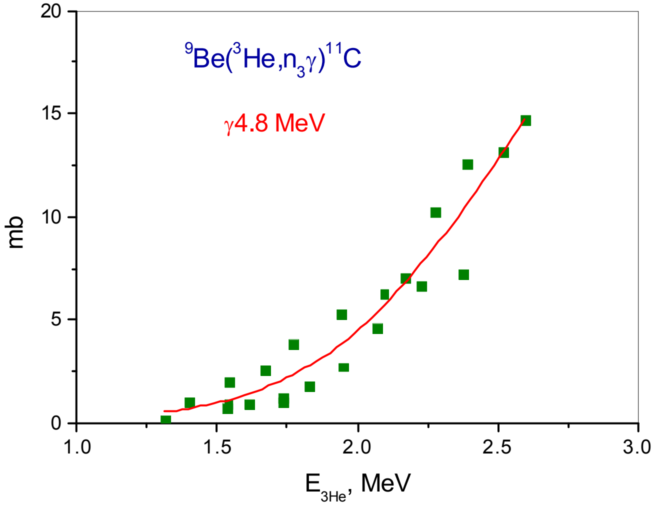

$^{9}Be(^{3}He,n_3\gamma)^{11}C$
γ4.8 MeV
mb
E_{3He}, MeV

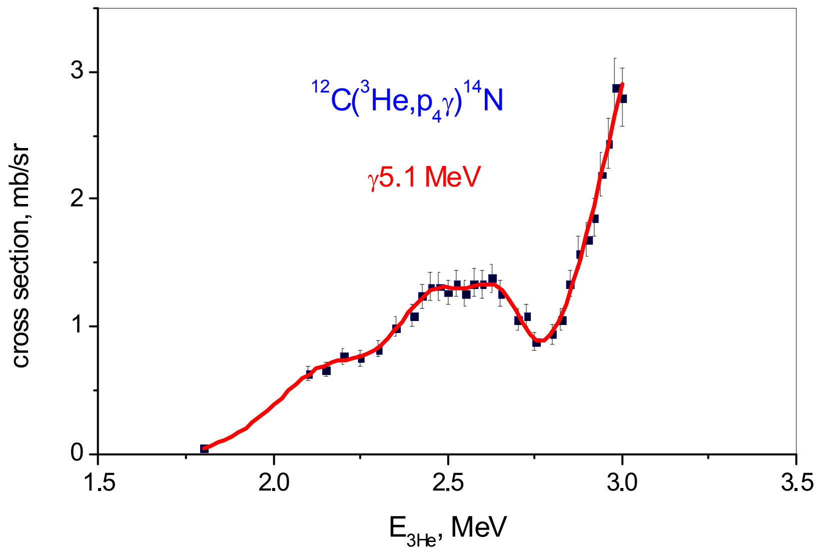

$^{12}C(^3He,p_4\gamma)^{14}N$
γ5.1 MeV
cross section, mb/sr
0
1
2
3
1.5
2.0
2.5
3.0
3.5
E_{3He}, MeV

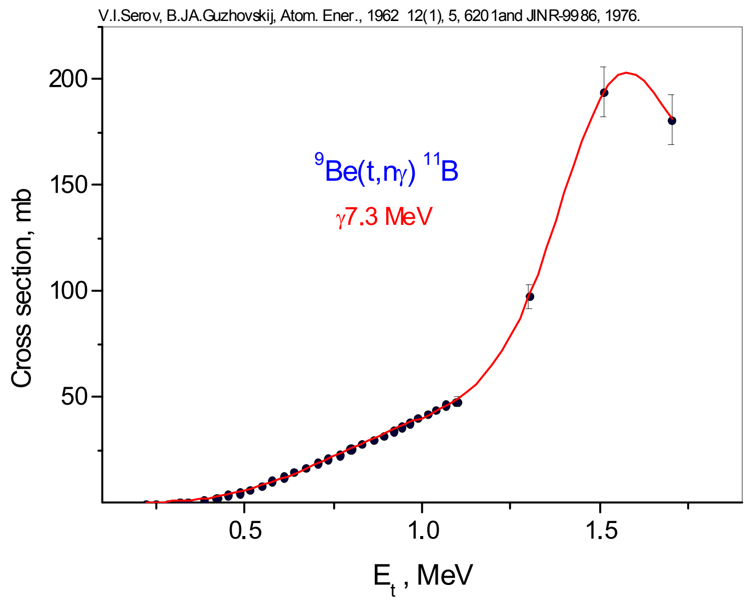

V.I.Serov, B.JA.Guzhovskij, Atom. Ener., 1962 12(1), 5, 6201and JINR-9986, 1976.
$^9Be(t,n\gamma)\ ^{11}B$
γ7.3 MeV
Cross section, mb
50
100
150
200
0.5
1.0
1.5
E_t , MeV

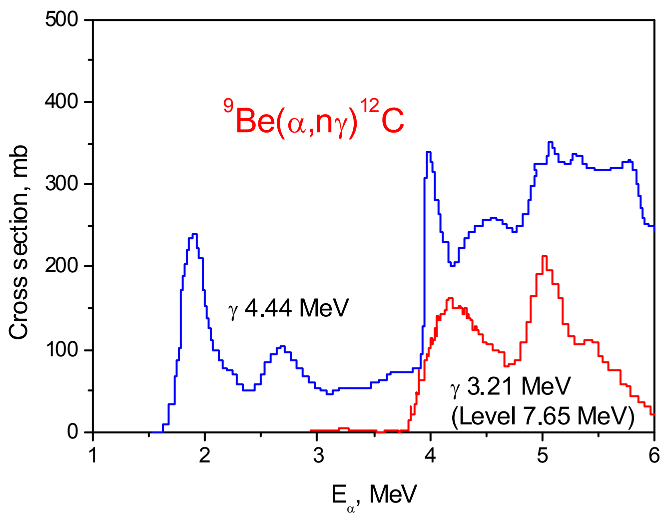

$^9Be(\alpha,n\gamma)^{12}C$
γ 4.44 MeV
γ 3.21 MeV
(Level 7.65 MeV)
Cross section, mb
0
100
200
300
400
500
1
2
3
4
5
6
E_α, MeV

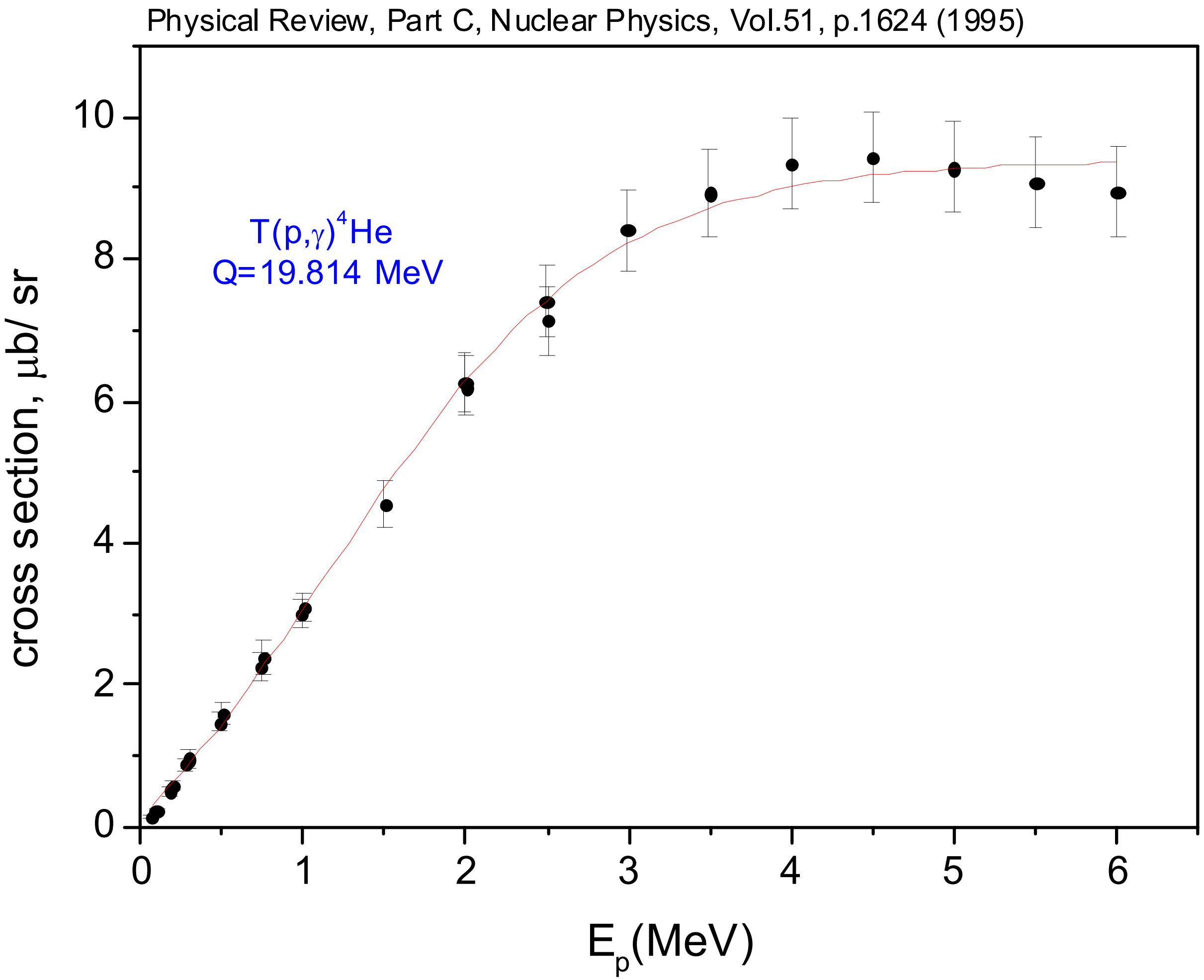
Physical Review, Part C, Nuclear Physics, Vol.51, p.1624 (1995)
T(p,γ)4He
Q=19.814 MeV
cross section, μb/ sr
0
2
4
6
8
10
0
1
2
3
4
5
6
Ep(MeV)

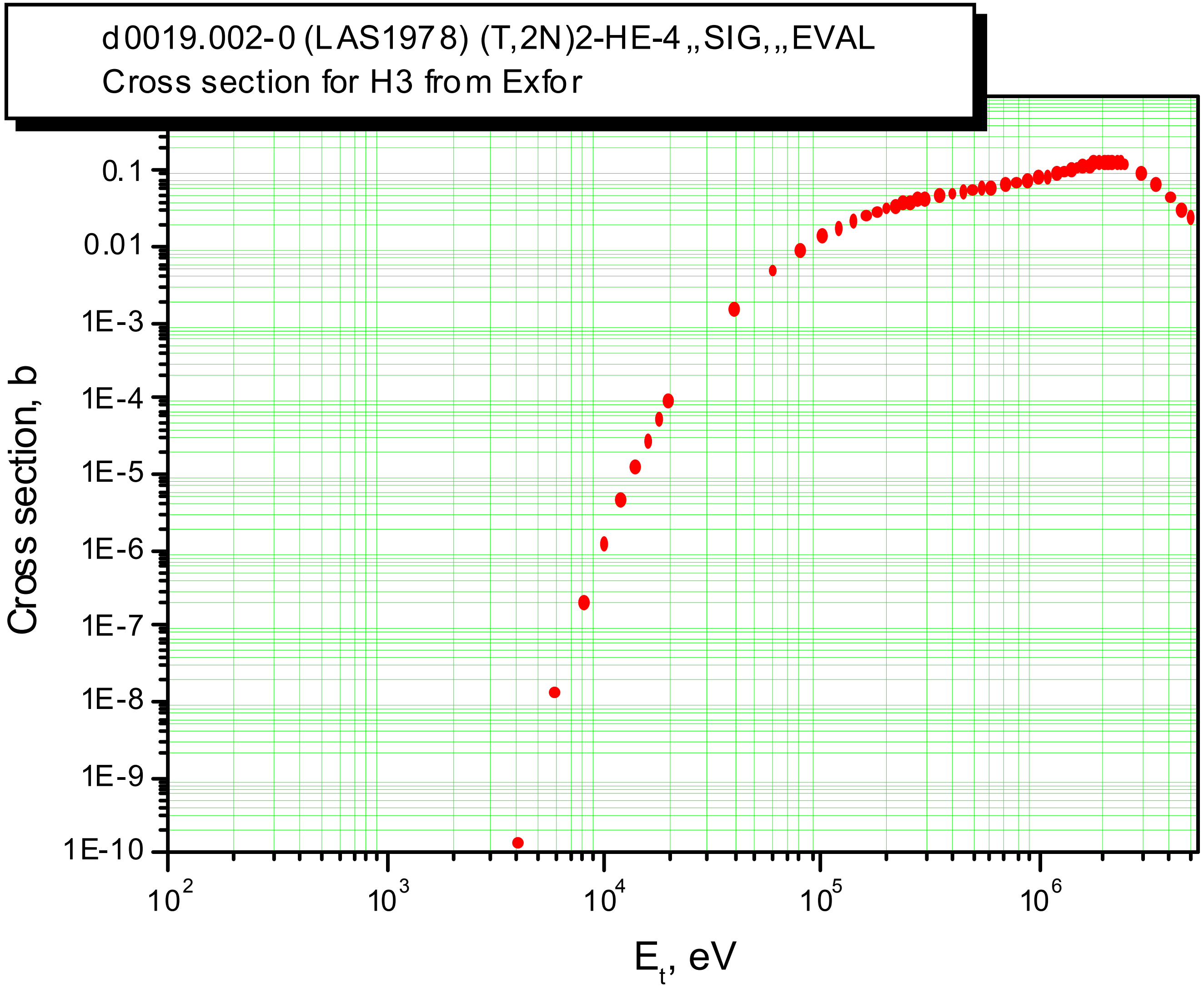
d0019.002-0 (LAS1978) (T,2N)2-HE-4,,SIG,,,EVAL
Cross section for H3 from Exfor
Cross section, b
0.1
0.01
1E-3
1E-4
1E-5
1E-6
1E-7
1E-8
1E-9
1E-10
10^2
10^3
10^4
10^5
10^6
E_t, eV

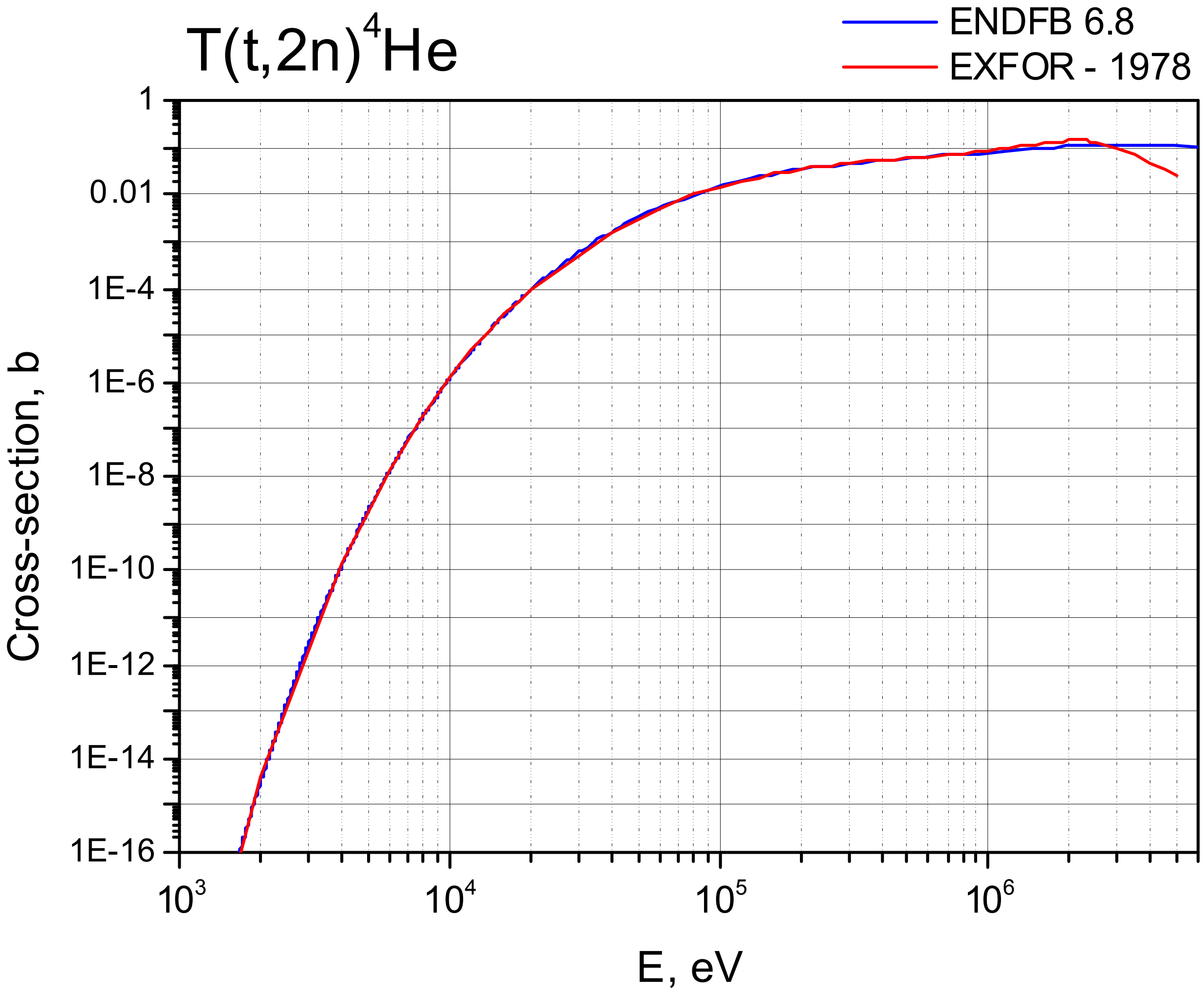
T(t,2n)4He
ENDFB 6.8
EXFOR - 1978
Cross-section, b
1
0.01
1E-4
1E-6
1E-8
1E-10
1E-12
1E-14
1E-16
10^3
10^4
10^5
10^6
E, eV

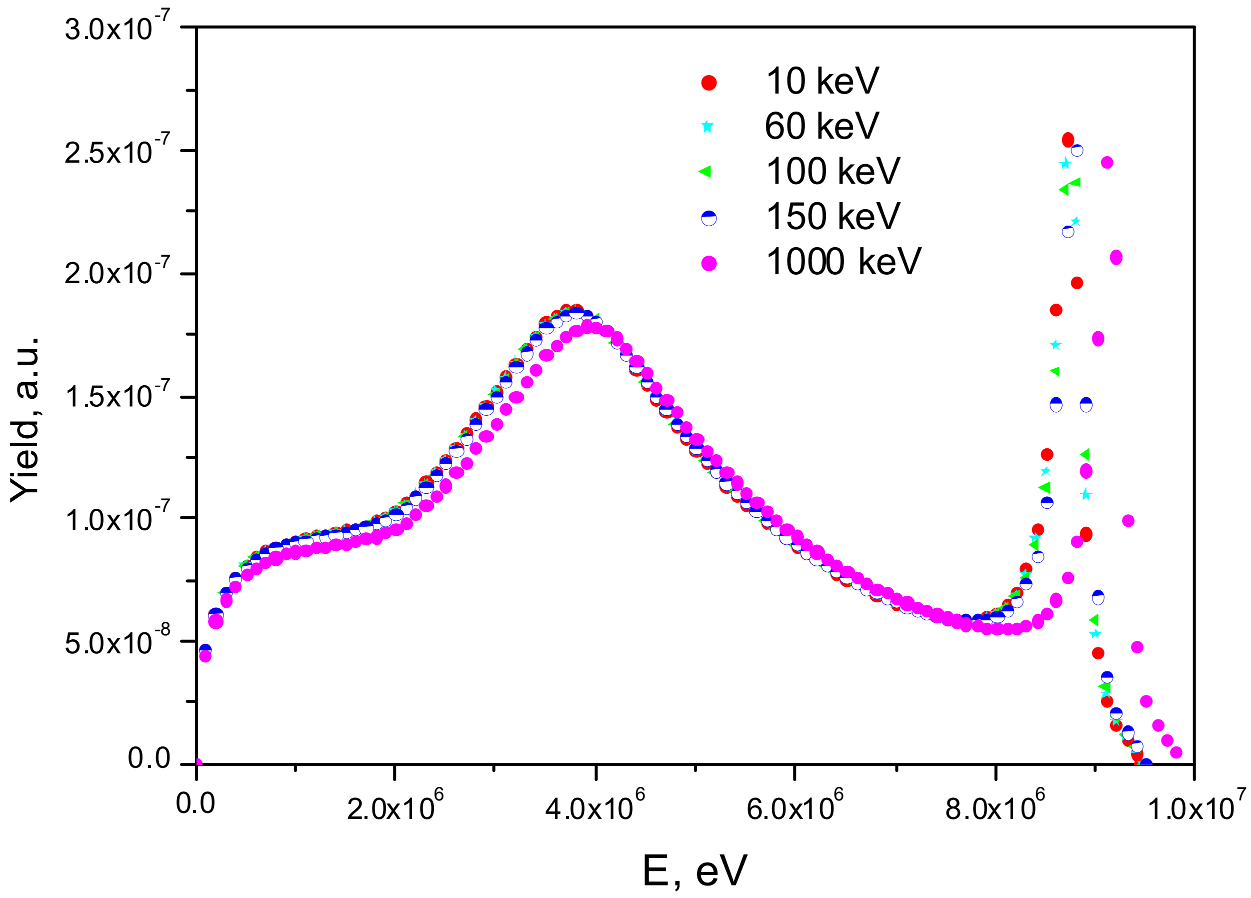

10 keV
60 keV
100 keV
150 keV
1000 keV
Yield, a.u.
E, eV
3.0x10^-7
2.5x10^-7
2.0x10^-7
1.5x10^-7
1.0x10^-7
5.0x10^-8
0.0
0.0
2.0x10^6
4.0x10^6
6.0x10^6
8.0x10^6
1.0x10^7